

Current Biology, Volume 27

Supplemental Information

**Functional Interactions between Newborn
and Mature Neurons Leading to Integration
into Established Neuronal Circuits**

Jonathan Boulanger-Weill, Virginie Candat, Adrien Jouary, Sebastián A. Romano, Verónica Pérez-Schuster, and Germán Sumbre

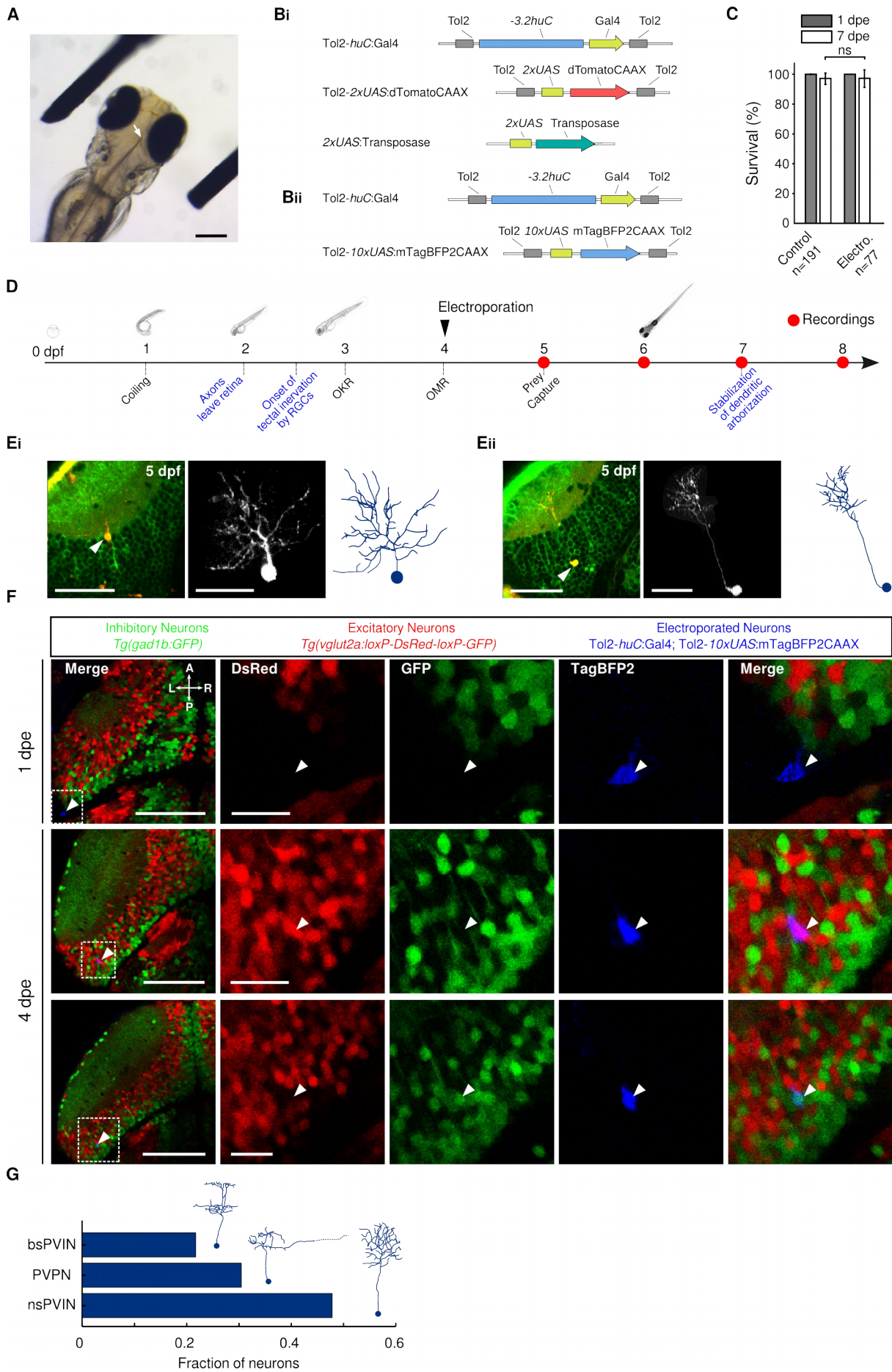


Figure S1 related to Figure 1. Morphological development and emergence of neurotransmitter identity of newborn neurons

(A) Picture of the electroporation preparation with the electrodes positioned on both sides of the larva. White arrow: the capillary containing DNA introduced in the tectal ventricle. Scale bar: 200 μm .

(B) i, DNA constructs used for labeling newborn neurons in *Tg(huC:GCaMP5G)*. Long-term expression of the vectors was achieved using the co-electroporation of a transposase enabling the stable incorporation of the constructs flanked with Tol2 sites, into the larva's genome. **ii**; Constructs used for labeling newborn neurons in *Tg(gad1b:GFP;vglut2a:loxP-DsRed-loxP-GFP)*.

(C) Quantification of the survival of electroporated larvae and age-matched controls, at 1 and 7 dpe. Note that electroporations did not show any significant effect in the survival of the larvae. ns.: $p > 0.05$.

(D) Time-course of the zebrafish larva development from 0 to 8 dpf, in terms of morphology, behavior and maturation of the visual system. Performing electroporations at 4 dpf enables studying the development of newborn neurons as they incorporate into an already functionally mature brain structure. OKR: optokinetic response and OMR: opto-motor response. Red dots: the developmental stages at which we performed the experiments. Arrow-head: the developmental stage at which we performed the electroporations.

(E) Two examples of mature neurons in 5 dpf larvae (**i** and **ii**). Left, position of the soma of the labeled neuron (arrow-head), within the PVZ layer of the optic tectum. Scale bar: 50 μm . Middle, a 3D projection of the mature neuron showing the neuron's morphology. Scale bar: 20 μm . Right, reconstruction of the neuron in the middle panel. Note that in contrast to the newborn-labeled neurons at 5 dpf (1 dpe), neurons far from the neurogenesis site already show mature morphologies. The neurons were labeled using single-cell electroporation in *Tg(huC:GCaMP5)* larvae.

(F) Examples of *Tg(gad1b:GFP;vglut2a:loxP-DsRed-loxP-GFP)* larvae electroporated with Tol2-*huC:Gal4* and Tol2-*10xUAS:mTagBFP2CAAX* constructs. Electroporated newborn neurons are indicated with white arrow-heads. Top, a newborn neuron not yet differentiated at 1 dpe. Middle and bottom, differentiated excitatory and inhibitory neurons at 4 dpe. First column: optical plane of

the optic tectum showing inhibitory (green), excitatory (red) neurons and a single newborn neuron (blue and arrow-head). Scale bars: 20 μm . Second, third and fourth columns, zoom of the dashed region in the first column, for the red, green and blue channels, respectively. Fifth column, all channels merged. Scale bars: 50 μm . L: left, R: right, A: anterior and P: posterior.

(G) Based on the morphology of the dendritic arbors at 4 dpe, newborn-labeled neurons developed into different neuronal types. Fraction of the different neuronal types. nsPVIN: non-stratified periventricular interneurons. PVPN: periventricular projection neurons. bsPVIN : bi-stratified periventricular interneurons.

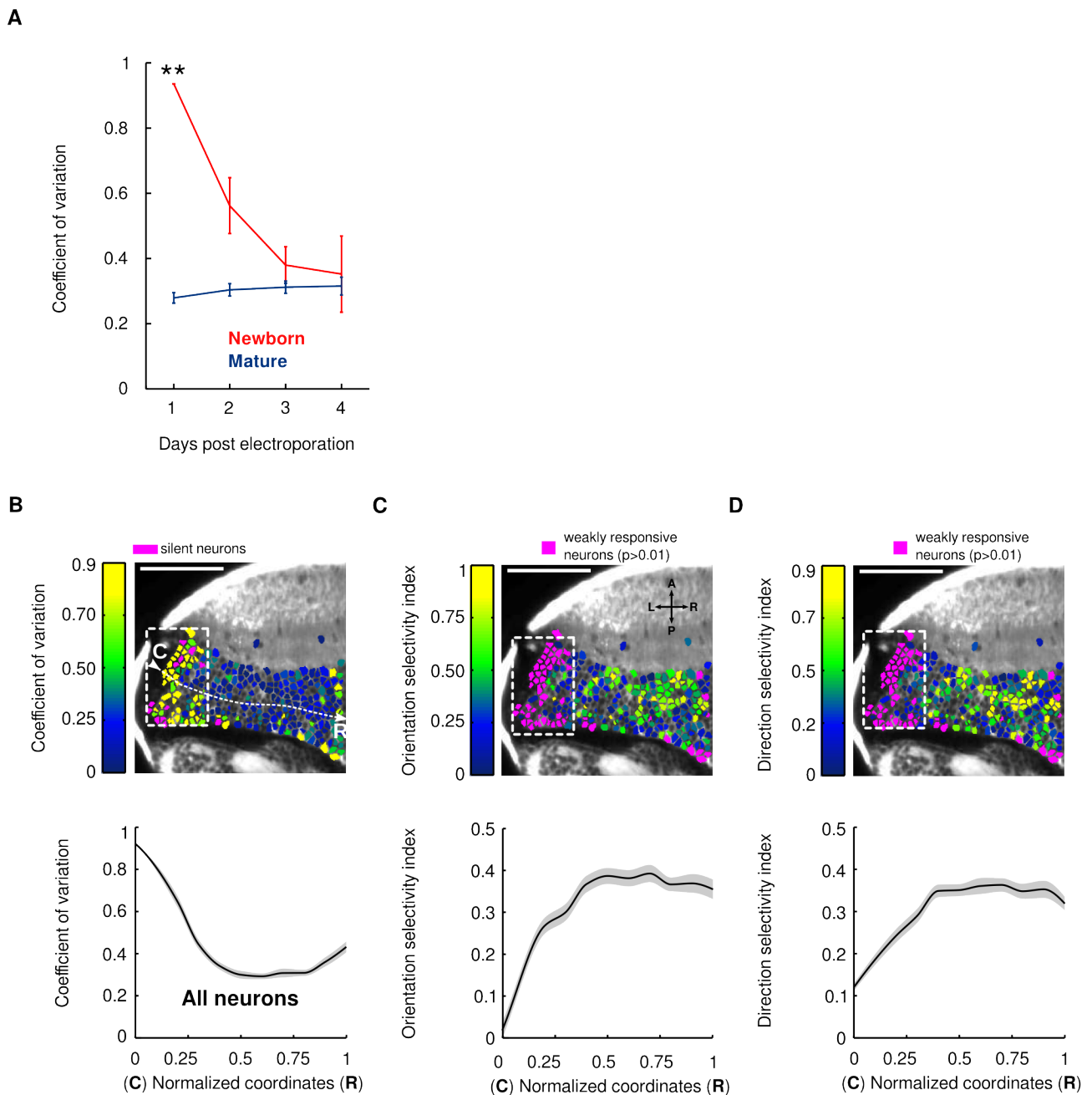


Figure S2 related to Figure 2. Development of functional intrinsic and visually induced properties of newborn neurons

(A) Development dynamics of the coefficient of variation of neuronal responses to drifting gratings, for newborn-labeled (red) and mature (blue) neurons (newborn-labeled neurons: $n=7, 10, 6$ and 3 , for 1-4 dpe, respectively; mature neurons: $n=973, 1340, 858$ and 453 mature neurons, from 5, 7, 4 and 2 larvae). **: $p < 0.01$. Error bars: SEM

(B-D) Top, example of an optical plane of the optic tectum with neurons color-coded according to

their coefficient of variation (B), orientation (C) and direction-selectivity index (D). Magenta: poorly responsive neurons (in C-D, $p > 0.01$, Mann-Whitney U tests or silent neurons in B). Note that these neurons were mainly clustered in close vicinity of the neurogenesis region (dashed area). Neurons with noisy baseline were left unlabeled. Arrows: orientation of the larva: L: left, R: right, A: anterior and P: posterior. Scale bar: 50 μm . Bottom, averaged distributions of the measured parameters on top, across the normalized coordinates along the caudo-rostral axis (white dashed curve on top, C: caudal, R: rostral), for all neurons, from 5 to 8 dpf ($n=5046$ neurons, from 18 larvae). Confidence interval: SEM. Changes in the orientation-, direction-selectivity index and coefficient of variation were significant across the caudo-rostral axis ($p=7.61 \times 10^{-20}$, $p=4.29 \times 10^{-23}$ and $p=4.57 \times 10^{-33}$, respectively, Kruskal-Wallis tests). Note the large differences for the three measured parameters close to the neurogenesis region (dashed region). Neurons involving few pixels (less than 5) or with unstable baselines (rapid changes generally indicating movement artifacts) were left unlabeled.

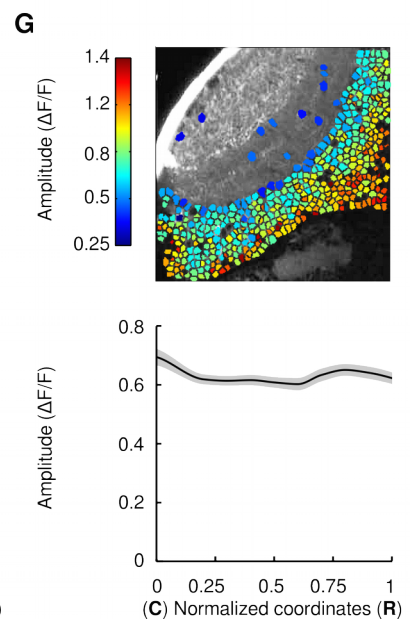
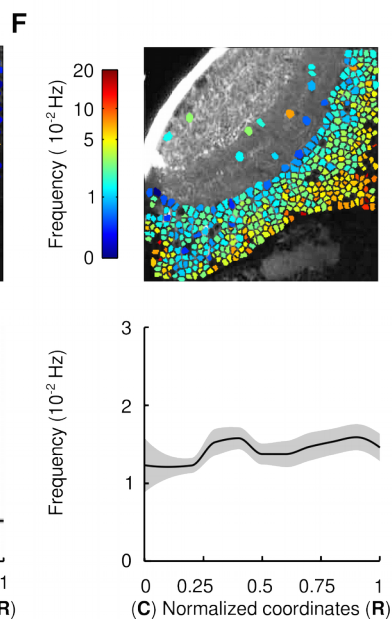
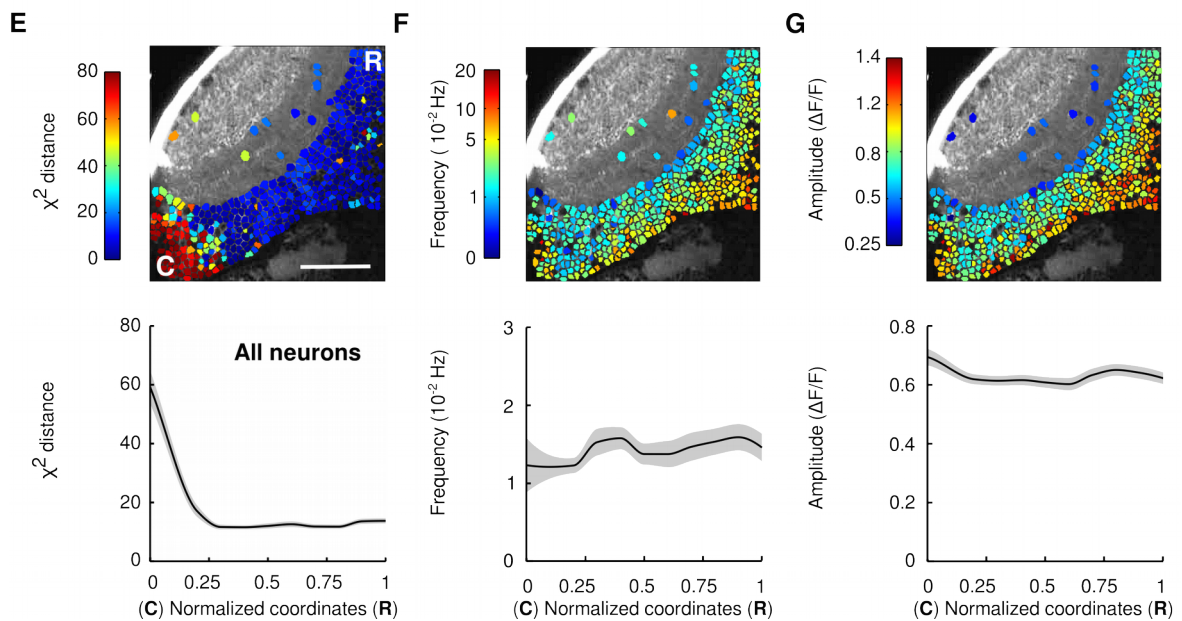
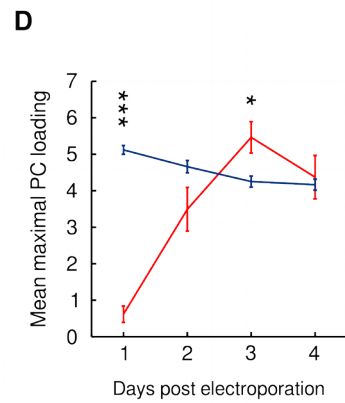
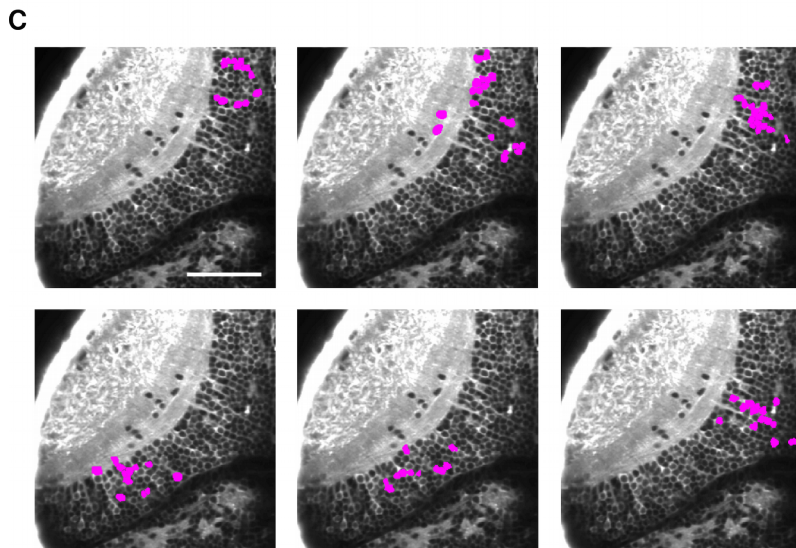
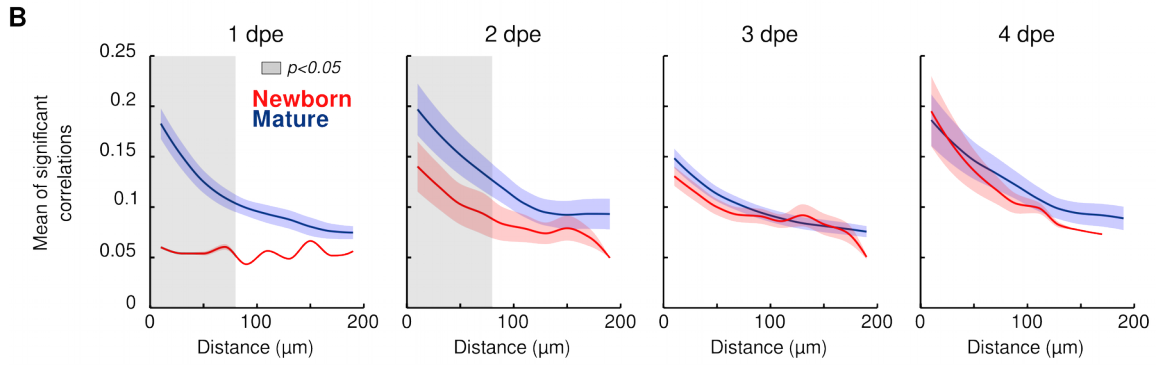
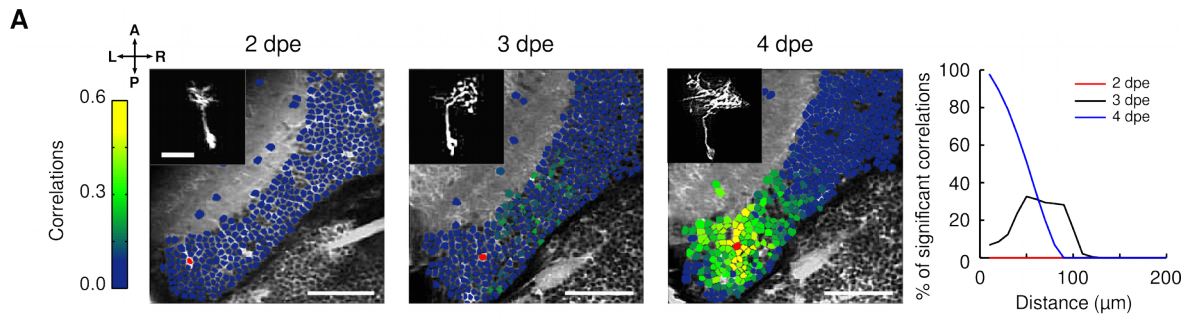


Figure S3 related to Figure 5. Spontaneous activity correlations between newborn-labeled and mature tectal neurons

(A) Left, example of an optical plane of the optic tectum containing a newborn-labeled neuron (red) chronically imaged from 2 to 4 dpe. Neurons are color-coded according to their pair-wise correlation values with the newborn-labeled neuron. Color scale bar: Pair-wise correlations between the newborn-labeled neuron and the rest of the tectal neurons. Scale bars: 50 μm . Insets: Morphology of the newborn-labeled neuron. Scale bars: 20 μm . Right, the percentage of significant correlations between the developing newborn-labeled neurons and the rest of the tectal cells, with respect to the physical distance between the neurons, for 2 (red), 3 (black) and 4 (blue) dpe. Neurons involving few pixels (less than 5) or with unstable baselines (rapid changes generally indicating movement artifacts) were left unlabeled.

(B) The developmental dynamics of the relationship between the mean of significant correlations and the physical distance between the neurons, for the newborn-labeled neurons (red) and the mature neurons (blue), from 1 to 4 dpe. Confidence intervals: SEM. Gray shaded areas: significant differences between newborn and mature curves ($p < 0.05$, Mann-Whitney U tests).

(C) Examples of 6 spontaneous neuronal assemblies showing their topographies. Magenta: neurons within an assembly.

(D) The maximal principal component loadings for newborn-labeled and mature neurons. Maximal principal component loadings reflect the level of prediction of the activity of a neuron by the activity of the assembly which contains it, assuming that each neuron belongs only to one assembly. *: $p < 0.05$. ***: $p < 0.001$. Error bars: S.E.M, newborn neurons: $n = 6, 15, 21, 15$; mature neurons: $n = 1962, 3564, 5296, 3969$, from 6, 10, 17 and 11 larvae, respectively.

(E-G) Top, example of an optical section of the optic tectum showing neurons color-coded according to X^2 distance (high values indicate low level of significant correlations), the frequency of the spontaneous Ca^{2+} events (middle), and the amplitude of the spontaneous Ca^{2+} events (right). The X^2 distance is the euclidean distance between the average distribution represented in **Figure 5C** (mature neurons, blue curve) and the distribution of each neuron, for distances shorter than 60 μm . High X^2 values indicate neurons that are isolated from others (do not show significant correlations with other neurons). Bottom, averaged distributions of the measured parameters, across the

normalized coordinates along the caudo-rostral axis, for all neurons, from 5 to 8 dpf (n=17678 neurons, from 44 larvae). Confidence interval: SEM. Changes in the X^2 distance across the caudo-rostral axis were significant, while the frequency and amplitude of the spontaneous Ca^{2+} events did not show significant changes ($p=4.12 \times 10^{-6}$, $p=0.55$ and $p=0.26$, respectively, Kruskal-Wallis tests). Neurons involving few pixels (< 5) or with unstable baselines (rapid changes generally indicating movement artifacts) were left unlabeled.

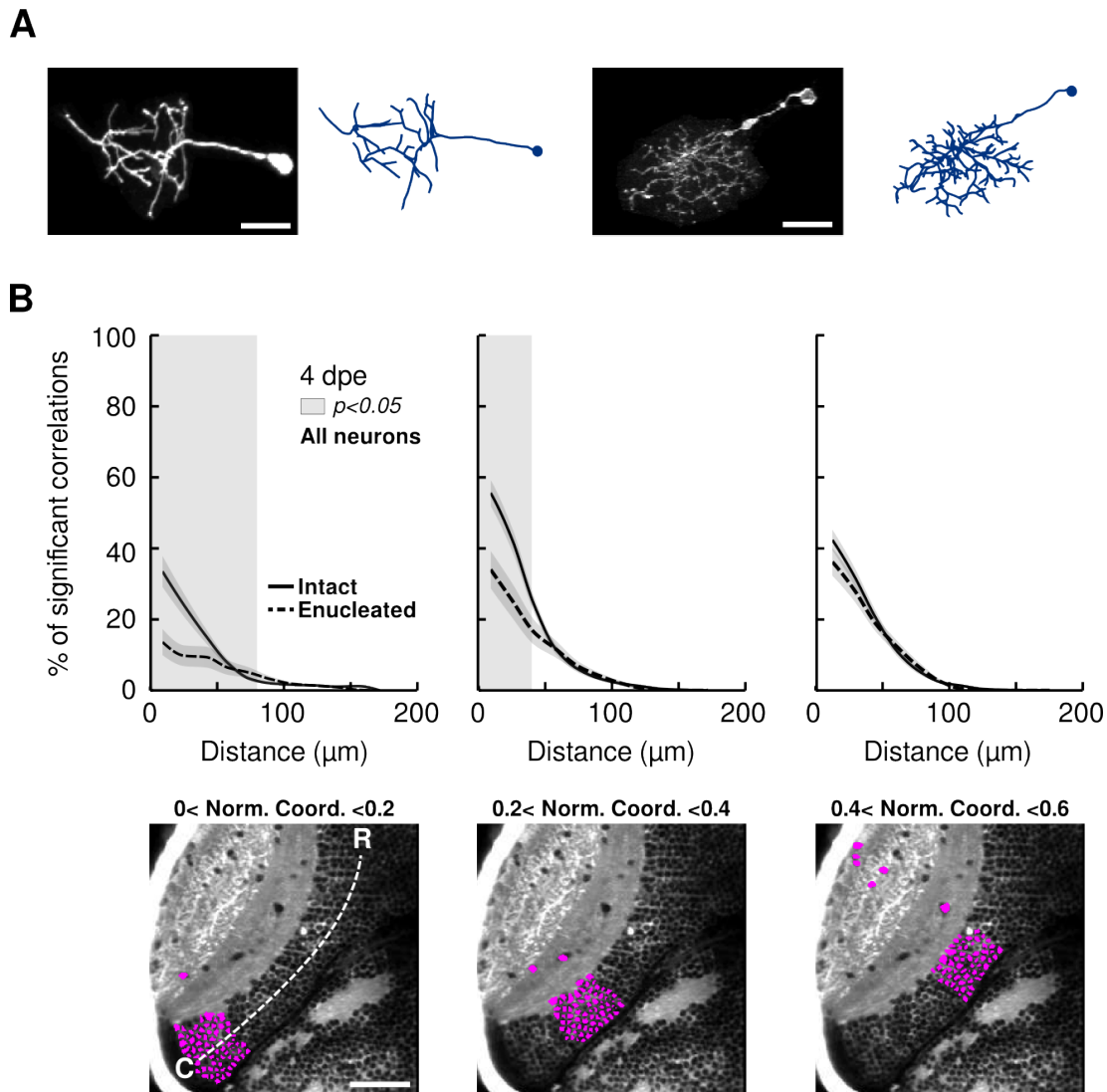


Figure S4 related to Figure 6. Enucleations prevent neurons from newborn neurons from incorporation into the mature tectal circuit but do not affect the development of their morphology.

(A) Two examples of the morphology of newborn-labeled neurons at 4 dpe after when enucleations were performed at 3.5 dpf. Left, a projection of the newborn-labeled neuron showing the developed dendritic morphology. Scale bar: 20 μm . Right, reconstruction of the neuron on the left.

(B) Top, the percentage of significant correlations with respect to the distance between neurons, at three different regions of the optic tectum (caudal, medial and rostral along the caudo-rostral tectal axis), at 4 dpe, for intact (solid line) and enucleated (dashed line) larvae. Bottom, an example of an optical section of the optic tectum showing the neurons (magenta) belonging to the three tectal regions (caudal: 0-0.2, medial 0.2-0.4, rostral: 0.4-0.6) used for the analyses in the top panel.

	Functionally mature neurons	Newborn-labeled neurons	Functionally immature neurons
1 dpe	161.7±19.4	37.9±22.6	138.8±24.3
2 dpe	353.7±61.7	72.0±11.9	309.9±61.6
3 dpe	194.0±29.0	159.6±78.2	175.6±30.2
4 dpe	157.6±7.6	65.7±20.8	149.4±11.0
Enucleated 4 dpe	106.3±9.1	55.2±15.2	92.6±8.5

Table S1 related to Figure 4 and 6. Number of significant spontaneous Ca²⁺ events for all experimental conditions. The average number of significant Ca²⁺ events during one-hour recordings and the standard error, for all experimental conditions (1 to 4 dpe in normal and enucleated larvae), for mature, newborn-labeled, and immature neurons. The difference in the number of events between the newborn-labeled and the functionally immature neurons partially contradicts **Figure S3F**. This difference could be explained by the fact that dTomato expression impeded the detection of low-magnitude Ca²⁺ events (due to quenching and/or cross talk between channels).